JOURNAL OF GEOPHYSICAL RESEARCH, VOL. 106, NO. C8, PAGES 16,815–16,823, AUGUST 15, 2001

Bubble entrainment by breaking waves and their influence on optical scattering in the upper ocean

Eric J. Terrill, W. Kendall Melville, and Dariusz Stramski

Scripps Institution of Oceanography, University of California, San Diego, La Jolla, California, USA

Abstract. Breaking waves at the ocean's surface inject bubbles and turbulence into the water column. During periods of rough weather the scales of wave breaking will increase with increasing sea states and result in mixing of the surface waters and the turbulent transport of bubbles to depth. Depending on their concentrations and size distribution, the entrained bubbles can significantly change the optical properties of water, introducing potentially significant errors in retrieval of remotely sensed hyperspectral data products. In this paper, the effects of bubbles on optical scattering in the upper ocean are investigated through optical scattering calculations based on field measurements of bubble populations. The field measurements were obtained offshore Point Conception, California, in June 1997, using an acoustical technique which measured the bubble size distribution at 2 Hz from a surface buoy designed to follow the longer waves. The effects of the bubbles on the bulk optical scattering and backscattering coefficients, b and b_b, respectively, are determined by using the acoustically measured size distributions, and size-dependent scattering efficiencies based on Mie scattering calculations. Time series of the bubble distributions measured in rough conditions (wind speed, $U_{10} = 15$ m/s, significant wave height, $H_{1/3} = 3.2$ m) suggest that the bubble contribution to light scattering is highly variable near the ocean surface, with values spanning roughly 5 decades over time periods of O(10) minutes. Bubble size distributions measured at a 0.7-m depth indicate that the optical effects of the bubbles on b_b, and hence the remote sensing reflectance, will be significant at bubble void fractions above 10^{-6} and that the bubble contribution to total b_b will exceed values of 10^{-2} m^{-1} inside bubble clouds.

1. Introduction

For the purposes of bio-optical analysis and remote sensing of ocean color, oceanic waters are often categorized as being either case 1 or case 2 water [*Morel and Prieur*, 1977]. Case 1 waters are those with optical properties that are determined primarily by chlorophyll pigments in phytoplankton and covarying derivatives such as grazing zooplankton and byproducts from the decay of both the phytoplankton and zooplankton. Case 2 waters are "everything else," for example, waters containing high concentrations of dissolved organic matter of terrestrial origin, mineral, and detrital particles from river runoff or resuspended sediments. These substances do not necessarily covary with local pigment concentration. Open ocean waters are usually considered as case 1, and coastal waters are often case 2. The existing algorithms for the interpretation of remotely sensed ocean color for case 1 waters are generally based on simple correlations between the ratios of water-leaving radiances at a few different wavelengths and the various quantities of interest, such as the chlorophyll concentration or the diffuse attenuation coefficient for irradiance. It is recognized that such algorithms usually perform poorly in case 2 waters. The task of developing robust bio-optical relationships and remote sensing algorithms for case 2 waters is significantly more complicated than for case 1 waters because of the wide variety of optically significant substances which vary independently of one another.

Paper number 2000JC000496.
0148-0227/01/2000JC000496$9.00

The classification into case 1 and case 2 waters ignores the fact that the optical scattering in the near-surface waters can be largely determined by air bubbles entrained by surface wave breaking. The concentration and size distribution of bubbles, the major determinants of their optical scattering, vary greatly in space and time and as a function of the synoptic wind and wave conditions. Consequently, a surface layer within any water body that would normally be classified as case 1 may show significant variations in scattering properties associated with intermittent bubble entrainment at moderate and high winds. Thus, in the presence of bubble entrainment, such water bodies will not satisfy the definition of case 1 water. Recognizing this limitation is important because vast areas of the ocean surface may experience significant bubble entrainment at any given time. In addition, the optical impact of bubbles occurs within the surface waters that have the most significant contribution to ocean color.

Bubbles can efficiently scatter light in water because their refractive index is considerably less than that of the surrounding medium and their size is typically large compared to wavelengths of light. The first assessment of the significance of bubbles for the scattering of light in the ocean was made by *Stramski* [1994]. These calculations were based upon historical measurements of concentrations and size distributions of bubbles measured in quiescent seas (no breaking waves). Therefore these calculations provide a lower limit of the bubble-induced light scattering from wave breaking (as opposed to biologically formed and stabilized bubbles that may dominate the bubble population during quiescent sea states). Stramski's early work demonstrated that even such conservative estimates

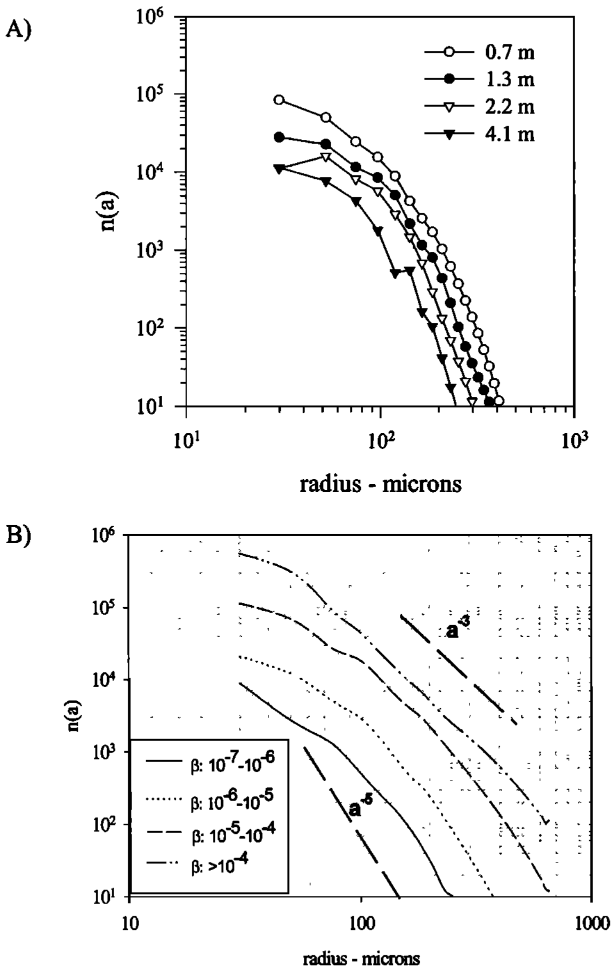

Figure 1. (a) An example of the bubble size distribution simultaneously measured in the field at four different depths (0.7, 1.1, 2.2, 4.1 m) during a large breaking event (near t = 700 s in the Point Conception data, Plates 1b and 1c. (b) Calculations of average bubble size distributions binned according to void fraction. Changes in the shapes of the distributions are a result of the temporal evolution of the bubble field.

of the bubble populations indicate nonnegligible contribution to the total scattering and backscattering coefficients of seawater (O(1) to O(10)%). The potential significance of bubbles to light scattering in the ocean has been supported in a more recent study, which analyzed both clean bubbles and bubbles coated with an organic film [*Zhang et al.*, 1998]. The coatings were shown to exert a small influence on total scattering by bubbles larger than 10 μm in size, but the estimated effect on backscattering was significant; that is, an enhancement of backscattering efficiency by as much as a factor of 4.

In this paper, we examine variations in the effects of bubbles from breaking waves on the bulk optical scattering and backscattering coefficients by using acoustically measured bubble size distributions and size-dependent scattering efficiencies based on Mie scattering calculations. Time series of the bubble distributions measured in rough conditions (wind speed U_{10} = 15 m/s, significant wave height $H_{1/3}$ = 3.2 m) are here used to illustrate strong fluctuations in light scattering near the ocean's surface due to the intermittent nature of bubble entrainment. A preliminary version of this paper was presented at the Ocean Optics XIV Conference held in Kona, HI in November 1998 [*Terrill et al.*, 1998].

2. Acoustic Bubble Measurements: Background and Field Data

2.1. Acoustical Instrumentation

The contrast in density and compressibility between a gas bubble and its surrounding fluid provides a mechanism for bubbles to both generate and interact with acoustic (pressure) waves, with bubbles resonating at characteristic frequencies that are defined by their radius. At acoustic frequencies much less than the resonant frequencies of the bubbles, the speed of sound is dependent solely on the volume of air present in the water, while at higher frequencies, bubble resonances cause the sound speed to become dispersive, dependent on the bubble size distribution. Improvements in our understanding of bubble acoustics now provide an effective description of the propagation of sound through a bubbly medium if the bubble size distribution is known [*Wildt*, 1946; *Clay and Medwin*, 1977; *Commander and Prosperetti*, 1989]. These advances in sound propagation theory allow oceanic bubble distributions to be determined acoustically using inversion techniques. The majority of the acoustical bubble measurement techniques recently reported [*Farmer and Vagle*, 1997, 1998; *Melville et al.*, 1997; *Terrill*, 1998; *Terrill and Melville*, 2000] are developments of techniques described by *Medwin* [1970, 1977], *Medwin et al.* [1975], *Medwin and Breitz* [1989], and *Medwin and Daniel* [1990], which involve the measurement of sound speed and attenuation over a range of frequencies (roughly corresponding to the resonant frequencies of bubbles present) and the inversion of the data for bubble size distributions. The most complete inversion algorithm is the procedure described by *Commander and McDonald* [1991] which includes off-resonant contributions.

The bubble measurements reported here were obtained with an acoustical technique to measure bubble size distributions using broadband pulse transmissions. While the measurement system is similar in principle to earlier systems, advances in technology have provided significant improvements in bandwidths and repetition rates. Sound speed and attenuation are measured over frequencies in the range 4 to 100 kHz, over path lengths of O(0.1–1) m, using pairs ("modules") of transmit and receive transducers. The resulting attenuation data is inverted for bubble radii in the range O(10–10^3) μm using the *Commander and McDonald* [1991] algorithm. The bubble size distribution is then used in a forward model to infer the sound speed as a function of frequency, which is tested against the directly measured sound speed. This internal consistency check provides an indication of the accuracy of the inverted distributions. The range of void fractions that the instrument will currently resolve ranges from O(10^{-8}) to O(10^{-4}). The broadband technique has been developed and tested in the laboratory against independent optical measurements of bubble size distributions generated using breaking waves in seawater and found to give excellent results [*Geissler and Jahne*, 1997; *Melville et al.*, 1997]. For a complete description of the acoustic instrumentation, the reader is referred to *Terrill and Melville* [2000].

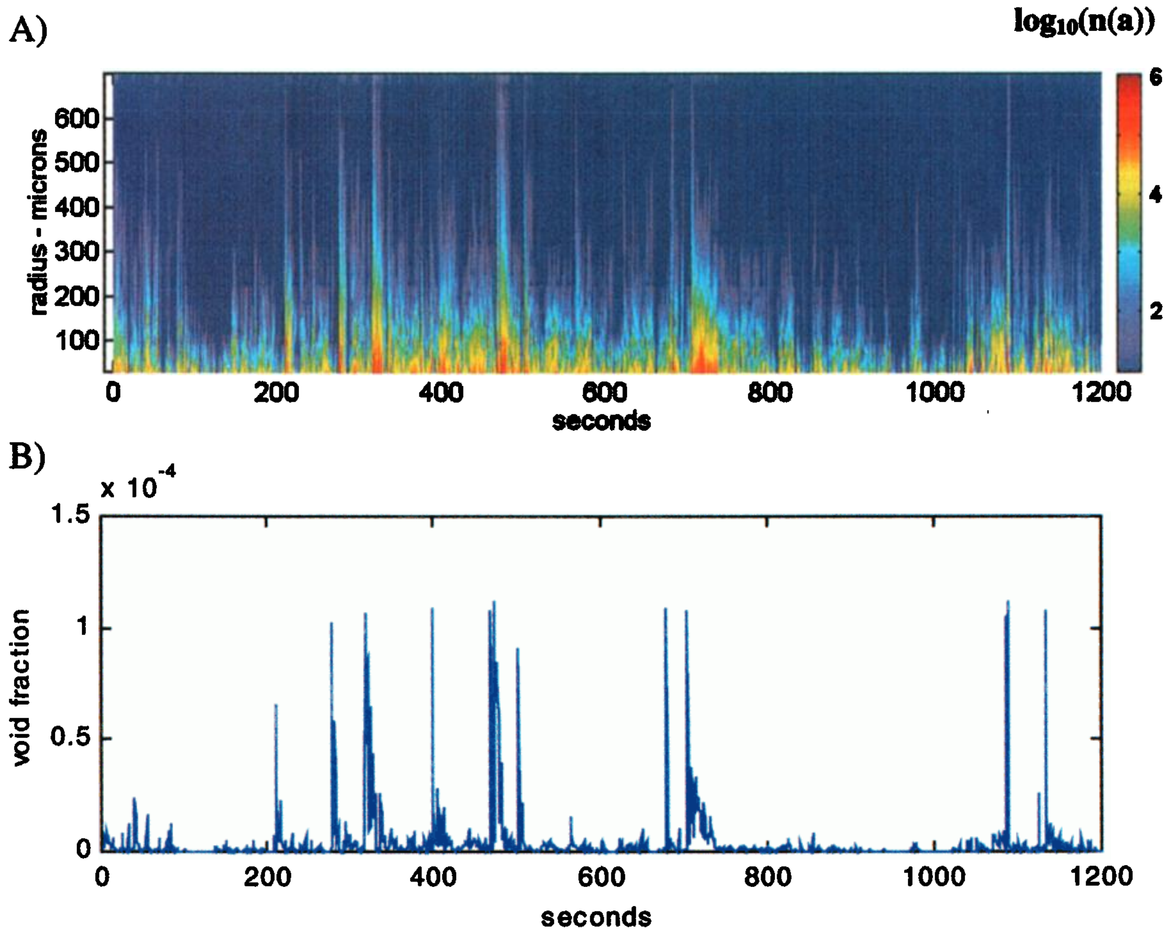

Plate 1. (a) A 20-min time series of bubble size distributions measured in the field near Point Conception, California, at a 0.7-m depth. Wind speeds were ~ 15 m s^{-1} and the significant wave height was 3.2 m. (b) The measured void fraction for the same 20-min record. Note the tendency for the bubble size distribution to extend to larger bubbles during periods of high-void fraction assumed to be wave breaking events.

2.2. Field Measurements

A field experiment designed to measure the near-surface bubble populations that result from wave breaking was conducted off Point Conception, California, in June 1997. A buoy was deployed with four acoustic bubble measuring modules mounted to a slender spar at distances 0.7, 1.3, 2.2, and 4.1 m below the sea surface. The spar was connected to the base of a surface float which housed the electronic hardware and data acquisition systems. Batteries onboard the buoy allowed autonomous operation for periods of O(1) day, after which it was recovered, serviced, and redeployed. The acoustic repetition rate of the system was 2 Hz for all the modules, providing acoustically inverted bubble sizes on a fast temporal scale.

To examine the effects of the injected bubbles on the scattered light, we consider a period of data that was acquired on June 5, 1997, when winds were a steady 15 m s^{-1} and the significant wave height was 3.2 m. Twenty minutes of bubble size distributions measured at a 2 Hz rate at the 0.7-m depth are shown in Plate 1a. The number density of the bubble size distribution n(a), (number of bubbles m^{-3} μm increment^{-1}), is given for the 30–800 μm size range that the system was configured for during the field measurements. (The bandwidth of the system has since been extended to size bubbles with radii ranging 15–1600 μm.) The high temporal resolution of the system resolves the intermittent nature of the bubble field, with a few large events giving distributions extending out to larger bubble sizes, and many more small events having fewer large bubbles. The void fraction of entrained air, defined as

$$\beta = \frac{4}{3}\pi \int a^3 n(a)\, da, \qquad (1)$$

is calculated for the bubble data presented in Plate 1b. The time series again shows the intermittent nature of the data, with void fractions changing several orders of magnitude over times of O(10) s. A typical example of the bubble size distributions at four different depths over an interval of 30 s inside a bubble cloud is shown in Figure 1a. These distributions are for the event that occurs near $t = 700$ s in the time series shown in Plates 1a and 1b.

Given the dynamics of the bubble cloud generation and the timescales of the physical processes which control their lifetimes (i.e., turbulent mixing, gas dissolution, Langmuir cells), it is clear that a long time-averaged representation of the bubble size distribution would not accurately reflect the true bubble populations present in the upper ocean. Ideally, one would like to understand the evolution of the size distributions as a function of the age of the entrained bubble cloud. Unfortunately, the nature of our field measurements prevents a direct determination of the age of the measured bubble populations as a

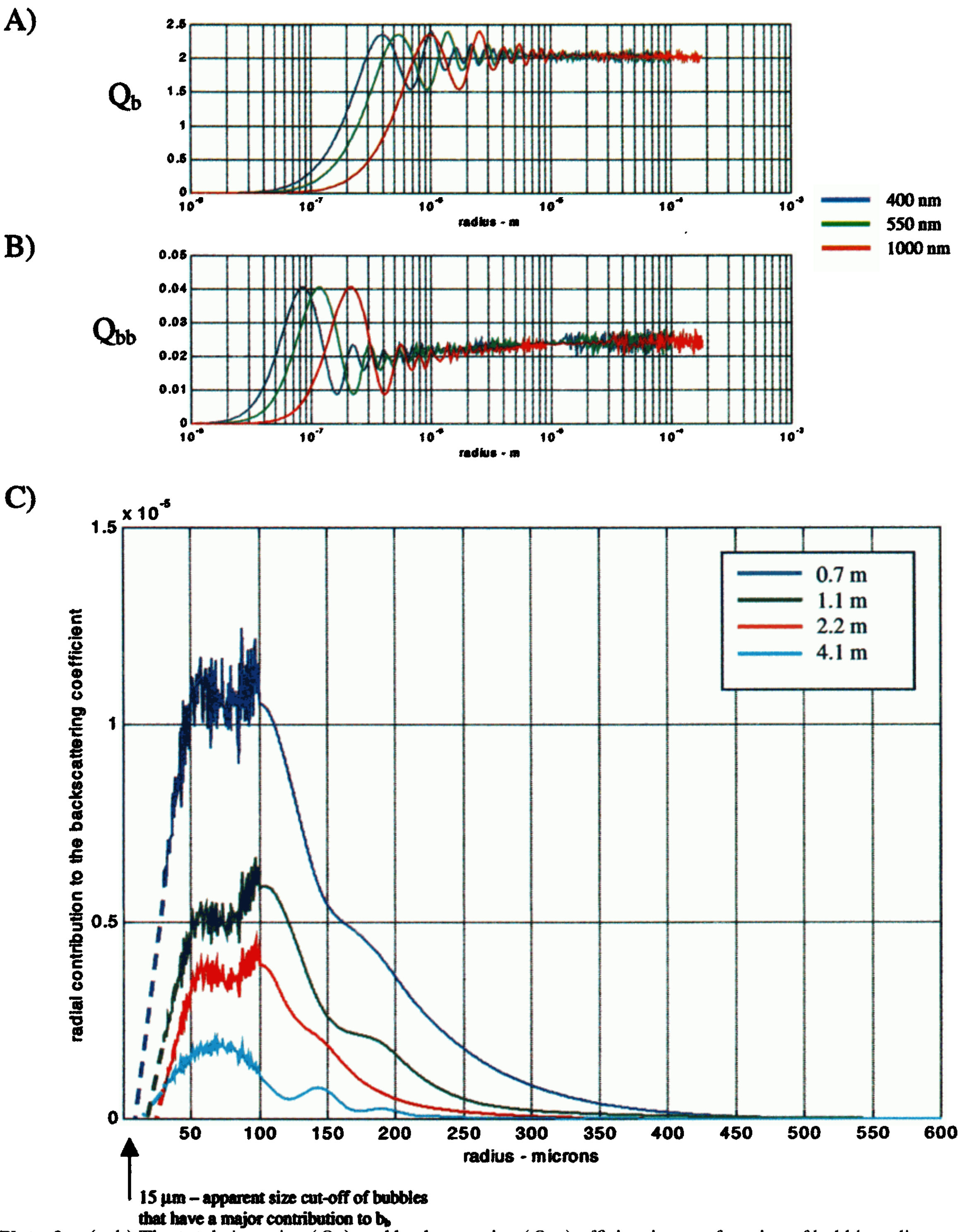

Plate 2. (a, b) The total scattering (Q_b) and backscattering (Q_{bb}) efficiencies as a function of bubble radius for light wavelengths of 400, 550, and 1000 nm. Note that the spectral dependence is negligible for bubbles with radii >4 μm for total scattering and 1 μm for the backscatter. (c) The contribution to the backscatter (b_b) as a function of bubble radius for the bubble size distributions measured at four depths offshore Point Conception, California (distributions shown in Figure 1a). The data suggest that bubbles with radii between 50 and 100 μm contribute the most to the bubble contribution to backscatter while extrapolation of the data to smaller radii suggests that radii smaller than 30 μm contribute <5% to the total bubble mediated backscatter.

function of the time since breaking, due in part to the advection of the bubbles past the acoustic sensors. This sampling constraint was emphasized by *Lamarre and Melville* [1992], who used underwater video and conductivity measurements of the void fraction to show that dense bubble clouds could have lifetimes of O(100) s as they advected past a fixed observer. However, we can learn something about the time dependence of the shape of the distribution if we consider the void fraction

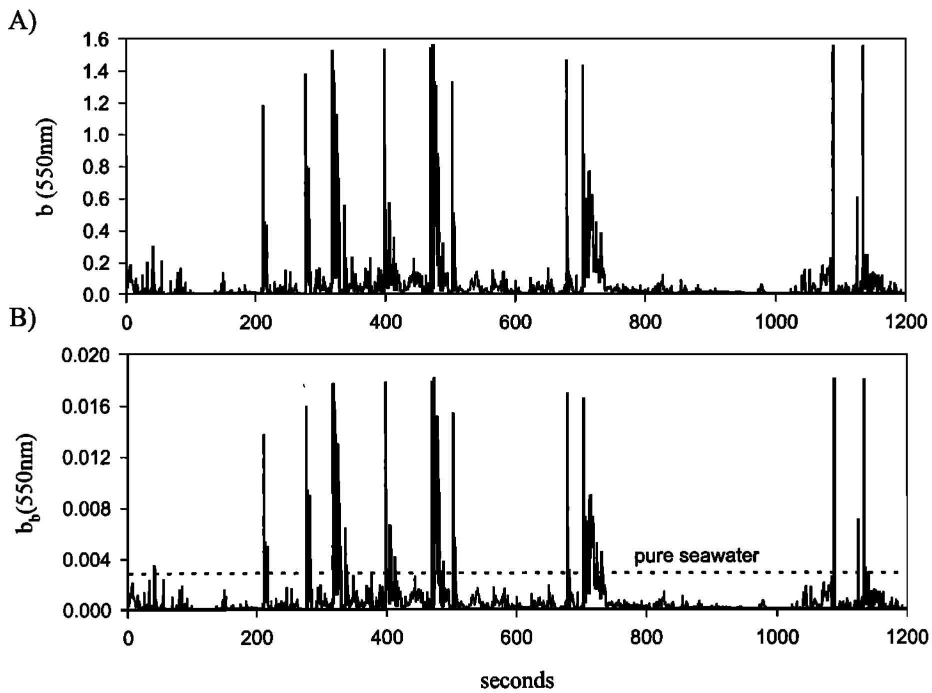

Figure 2. Twenty-minute time series of the (a) total scattering, b and (b) backscattering coefficients, b_b (light wavelength of 550 nm) calculated from the bubble data obtained off Point Conception, California, at a depth of 0.7 m. Note the episodic nature of the scattering coefficients due to the variable nature of the bubble densities.

of the mixture as a proxy for time. Under this simple assumption the higher void fractions would represent younger bubble distributions as compared to lower void fractions that are indicative of bubble clouds that have degassed for some time. Average bubble size distributions based on the previously shown data set, binned according to their void fraction in bins that span 1 order of magnitude are shown in Figure 1b. The binned data shows no universal shape of the bubble size distributions, a result of the physics of the radius-dependent bubble rise speed, turbulent mixing, and gas dissolution. Owing to both the intermittent nature of wave breaking and the time-dependent shape of the bubble size distribution, the effects of the bubbles on the inherent optical properties must be analyzed with temporal resolution commensurate with the dynamics which control their lifetimes.

3. Bubbles and Their Optical Properties

Light scattering from a single air bubble in water can be determined using Mie theory which allows for the solution of the angular distribution of light scattered from the bubble when illuminated by a monochromatic source. The Mie solution to the angular distribution of light scattering from a sphere can be summarized using scattering efficiency factors which describe the radiant energy either completely scattered into all directions, Q_b, or the energy backscattered, Q_{bb}, as a fraction of radiant energy intercepted by the projected area of the sphere. The backscattering efficiency is the more relevant for issues pertaining to bubble mediated effects on remotely sensed ocean color. Using an algorithm for homogenous spheres [*Bohren and Huffman*, 1983], scattering intensities where calculated for bubbles in water ranging in size from 0.01 μm to a few hundred microns using a relative refractive index of 0.75. Since the relevant parameter describing the size of the bubble in the Mie calculation is the bubble diameter relative to the wavelength of the incident light, $\pi D/\lambda$, calculations at one optical wavelength can be applied to other wavelengths through appropriate scaling. Plates 2a and 2b show both the total and backscattering efficiencies as a function of radius for light at wavelengths of 400, 550, and 1000 nm using the calculations of *Stramski* [1994]. Note that the spectral dependence of Q_b becomes negligible for bubbles with radii greater than 4 μm, while Q_{bb} has little spectral dependence for bubbles greater than 1-μm radius.

The contribution of a given particle size distribution to the bulk inherent optical properties can be calculated by treating the bubbly water as a mixture of random, single-scattering particles, whereby the bulk properties are the sum of the contributions by the individual bubbles [*Mobley*, 1994]. Hence the bulk scattering coefficient and backscattering coefficient for a given bubble size distribution are

$$b(\text{bubbles}) = \int Q_b \pi a^2 n(a)\, da, \tag{2}$$

$$b_b(\text{bubbles}) = \int Q_{bb} \pi a^2 n(a)\, da, \tag{3}$$

respectively. The limits of the integral are defined by the range of bubble radii present in the mixture and are typically numerically integrated using 1-μm increments in bubble radius.

The contribution to the backscattering coefficient $b_b(550)$, as a function of radius, is calculated for the example bubble size distribution in Figure 1a and presented in Plate 1c. The area under the curve is the integral of (3). The curves suggest that bubbles with radii ranging from ~50–150 μms appear to

A)

B)

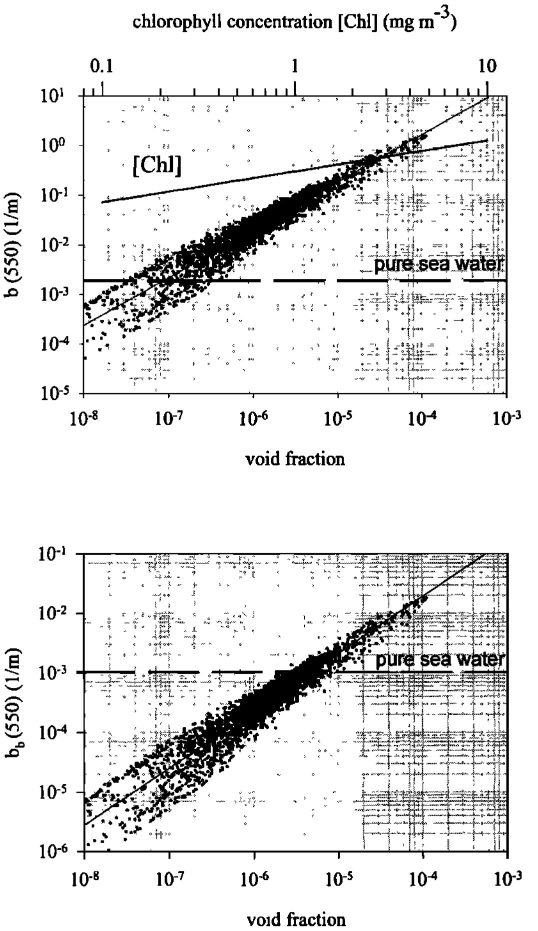

Figure 3. Scatterplots of (a) b and (b) b_b versus the void fraction of the bubble density. Shown for reference are the scattering coefficients for pure seawater. The data strongly suggest that the optical effects of the bubbles on b_b, and hence the remote sensing reflectance, will be significant at void fractions above 10^{-6}. The variability in the optical field expected from the bubbles is put into context if the bubble data shown in Plate 1 are considered. Reference values for pure sea water scatter at 550 nm [*Smith and Baker*, 1981] are shown. Also presented in Figure 3a is the empirical relationship between scatter at 550 nm and [Chl] for case 1 waters from *Loisel and Morel* [1998]. See text for a description of this relationship.

contribute to the majority of the backscattering coefficient, with the peak in the curve occurring at ~60–70 μms followed by significant rolloff at the smaller radii. While the measured bubble size distributions cut off at 30 μm, extrapolating the backscattering contribution curves to smaller radii (the dashed lines in Plate 2c) suggests that the smaller bubbles contribute only a small percentage of the total optical backscattering coefficient over the range of bubble densities and sizes expected when waves are breaking at the ocean surface. Assessment of other measured distributions exhibited similar trends. The contribution by bubble radius to the total scattering coefficient, b, also revealed the relative unimportance of the optical properties of the very small bubbles (when compared to the bubbles of radius O(10–100) μm) for the bubble size distributions present during active wave breaking conditions. Since the scattering efficiencies Q_b and Q_{bb} have little spectral dependence at bubble sizes greater than 4 and 1 μm, respectively, the calculations also suggest that bubble mediated effects on the scattering and backscattering coefficients will have little spectral dependence.

The temporal variability of the bubble-mediated optical scattering is evident in the time series of b and b_b generated using (1) and (2) and the field data already discussed. The time series are calculated for an optical wavelength of 550 nm and shown in Figures 2a and 2b. The time series of $b_b(550)$ contains several high scatter events that correlate with periods of high bubble densities. During many of these events, b_b is determined to exceed the value for pure seawater for durations lasting up to tens of seconds. To assess the correspondence between the bubble densities and the bubble contribution to the bulk scattering properties, scatterplots of the void fraction versus b and b_b (Figures 3a and 3b) are shown. Twenty-four hundred data points (20 min of data) are shown on a log-log scale and reference lines representing the values for pure seawater scatter at 550 nm [*Smith and Baker*, 1981] are displayed. Pure seawater is defined here as waters that are devoid of dissolved and suspended particulate matter, and the corresponding scattering values of *Smith and Baker* [1981] represent molecular scattering.

The extreme range of scattering levels due to the bubbles is clearly evident in the plots, with the values spanning a range of 5 decades for only 20 min of data, with b ranging from O(10^{-5}) to over 1 m^{-1}, and b_b from O(10^{-6}) to over O(10^{-2}). The comparison of the levels of b and b_b with the values for pure seawater provides a clear indication of when the bubble densities may become optically significant. For example, the data suggests that the level of bubble contribution to backscatter becomes significant at bubble densities with void fractions above 10^{-6}.

The relevance of entrained bubbles to optical scattering in the ocean can also be assessed if commonly accepted relationships between the light scattering coefficient due to particles, b_p, and chlorophyll a concentration, [Chl], are examined for open ocean (case 1) waters [e.g., *Morel*, 1980; *Gordon and Morel*, 1983]. These empirically derived relationships are commonly used in bio-optical models in which levels of [Chl] can range from very low values of ~0.02 mg m^{-3} up to 20 mg mg m^{-3} or more, depending on whether the waters are oligotrophic or eutrophic. Recently, *Loisel and Morel* [1998] have reexamined a large number of bio-optical data sets in open ocean waters to determine empirical relationships between the optical beam attenuation due to particles c_p, and [Chl]. Since the authors express the regressions for the beam attenuation coefficient rather than the scattering coefficient, the absorption due to particles needs to be subtracted to determine the scattering values b_p. Using data from long time series stations near Bermuda and Hawaii (BATS and HOTS sites), as well as data from a number of cruises in the tropical Atlantic and Pacific Oceans, the authors determine a regression for the optically homogenous surface layer to be

$$c_p(\lambda) = (660/\lambda)0.252[Chl]^{0.635}, \qquad r^2 = 0.76. \qquad (4)$$

To obtain values for $b_p(550)$ as a function of [Chl], the absorption a_p is subtracted,

$$b_p(550) = c_p(550) - a_p(550), \qquad (5)$$

where

$$a_p(550) = 0.011825*[Chl]^{0.8385428} \qquad (6)$$

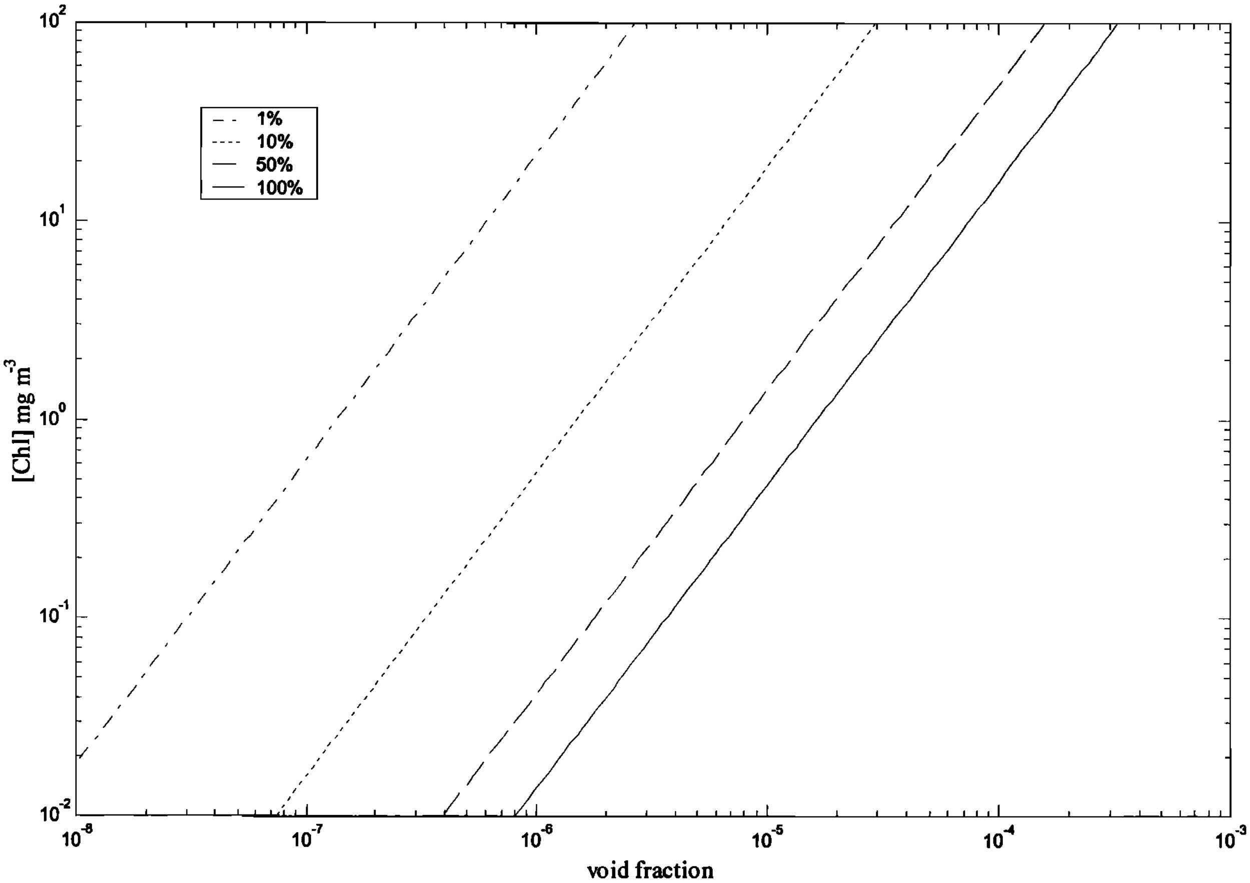

Figure 4. Estimates of the contribution of total optical scatter due to entrained bubbles relative to accepted chlorophyll ([Chl]) scatter relationships for open ocean (case 1) waters. For a given [Chl] concentration, the lines indicate at which bubble void fraction the bubbles have an optical scatter 1, 10, 50, and 100% of the scatter induced by the chlorophyll. Clearly, oligotrophic waters with low [Chl] concentrations may be susceptible to large errors in the bio-optical interpretation of the scatter measurements if air bubbles are present.

is a relationship relating [Chl] to the particulate absorption coefficient a_p [*Bricaud et al.*, 1998]. The results of these calculations are shown for comparison with the bubble induced optical scatter on Figure 3a. Clearly, for case 1 waters the bubble contribution to total scatter may be a significant fraction of the contribution by particles, dependent, of course, on the respective levels of the two constituents. For example, in oligotrophic surface waters that have low [Chl], the errors in the bio-optical interpretation of measured optical properties may be very large if the surface waves are breaking. While usually associated with moderate to high wind speeds, breaking may also result from wave-wave and wave-current interactions [*Melville*, 1996].

To aid in the estimate of the possible errors that may result from applying the optical scatter versus [Chl] relationships to regions where wave breaking may be present, the percentage of scatter that results from bubbles, relative to [Chl]-dependent particle scattering, is determined for a wide range of bubble and chlorophyll densities and shown in Figure 4. To perform these calculations, a regression of the bubble-induced optical scatter as a function of bubble void fraction (data shown in Figure 3b) was generated (based on the logarithms of the data),

$$b(550) = 11481.5(9.14^{\log_{10}(\beta)}), \qquad r^2 = 0.95, \qquad (7)$$

and compared with the relationships for particle scattering already discussed. The curves in Figure 4 demonstrate again that the scatter due to bubbles may be significant relative to the scatter by particles, depending of course on the relative concentrations of the two. For example, at a void fraction of 10^{-6}, scatter from bubbles is almost as large as the scatter by particles at a low [Chl] of ~0.02 mg m^{-3}, while in more productive waters with [Chl] levels at 0.5 mg m^{-3}, scatter from the same bubble density is only ~10% of the scatter from particles (the chlorophyll). However, if the void fraction is increased an order of magnitude to 10^{-5}, the bubble scatter is about equal with that of particles.

4. Discussion and Conclusions

The effect of bubbles on the inherent optical properties of the upper ocean have been estimated by applying Mie scattering calculations to high-resolution bubble data obtained from a recently developed acoustic technique. They are the first known calculations of the fluctuations in the inherent optical properties that are based upon bubble measurements obtained with sufficient temporal resolution to resolve the variability of the bubble field. The calculations should provide a cautionary note when analyzing either in situ or remotely sensed optical data obtained in high sea states characterized by breaking

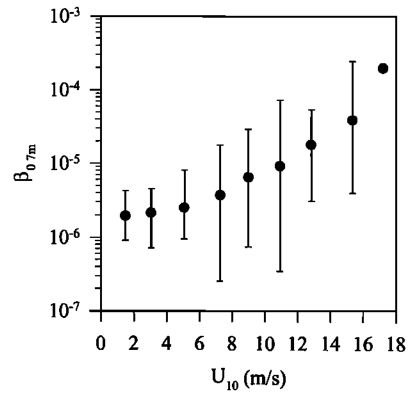

Figure 5. Dependence of the mean air void fraction measured at 0.7-m depth versus 10 m wind speed as measured in the North Atlantic over the winter of 1993–1994 during the ASREX experiment (see *Terrill and Melville* [1997] and *Terrill* [1998] for details of experiment). Solid circles represent averages of the data grouped with 2 m s^{-1} bins, and the error bars are the scatter in the measurements. Empirical relationships based on long time series can be used to assess when wave breaking will inject sufficient quantities of air into the water column to be optically significant.

waves. The numbers should also be considered as lower bounds since much higher bubble void fractions are known to exist at shallower depths directly beneath breakers. For example, the measurements by *Lamarre and Melville* [1992] have shown void fractions can reach levels of O(1–10)% at depths <0.5 m, with the events generally lasting less than 1 s. When these transient high-void fractions are cautiously extrapolated using the optical scattering levels shown on Figures 3a and 3, the data suggests that scattering levels of O(1–10) m^{-1} are easily attainable. Furthermore, if the assumptions of *Zhang et al.* [1998] are correct regarding the role of organic films in coating bubbles and enhancing their ability to scatter light, the levels of bubble mediated optical scatter suggested in this work may actually underestimate the true scattering values.

While the calculations for the effect of bubbles on the bulk inherent optical properties cannot be considered a substitute for in situ measurements of light properties, the analysis suggests that bubble-mediated effects on the upper ocean light scattering properties will be significant and highly variable during rough sea states. The synoptic oceanographic conditions under which wave breaking injects sufficient quantities of bubbles for them to become optically significant remains a difficult question to answer since the dynamics and statistics of ocean wave breaking and air entrainment are still poorly understood (see review by *Melville* [1996]). An initial assessment can be made if we consider in situ measurements of air entrainment during a separate field experiment conducted in the winter of 1993–1994. During this experiment an autonomous buoy system with a vertical array of sound speed modules designed to sample the void fraction at a 2-Hz rate, was moored in the North Atlantic (ASREX experiment [*Terrill and Melville*, 1997; *Terrill*, 1998]). The dependence of the average void fraction at 0.7-m depth (computed using 40-min records) on the average wind speed that was measured over the 43 days of the experiment is shown in Figure 5. Despite the scatter in the data the wind speeds during which bubbles may become optically significant is put into context if the calculations for the scattering coefficients b and b_b (again refer to Figure 3) are considered. The variability in the upper ocean bubble field which results from the complexity of wave breaking, coupled with the uncertainty in the assumptions used in bubble light scattering calculations, indicates that field research efforts involving both simultaneous bubble and optical scattering measurements are required to better understand the role of oceanic bubble distributions in remotely sensed ocean color data.

Acknowledgments. The National Science Foundation (Ocean Instrumentation grant OCE 95-29808) and the Office of Naval Research Acoustics (grant N00014-98-1-0150) and Environmental Optics (grant N00014-99-1-0223) divisions are acknowledged for support of the development and testing of the acoustic bubble sizing instrumentation and the subsequent analysis of the field data described in this paper.

References

Bohren, C. F., and D. R. Huffman, *Absorption and Scatterng of Light by Small Particles*, John Wiley, New York, 1983.
Bricaud, A., A. Morel, M. Babin, K. Allali, and H. Claustre, Variations of light absorption by suspended particles with chlorophyll a concentrations in oceanic (case 1) waters: Analysis and implications for bio-optical models, *J. Geophys. Res.*, *103*, 31,033–31,044, 1998.
Clay, C. S., and H. Medwin, *Acoustical Oceanography*, John Wiley, New York, 1977.
Commander, K. W., and R. J. McDonald, Finite-element solution of the inverse problem in bubble swarm acoustics, *J. Acoust. Soc. Am.*, *89*, 592–597, 1991.
Commander, K. W., and A. Prosperetti, Linear pressure waves in bubbly liquids: Comparison between theory and experiments, *J. Acoust. Soc. Am.*, *85*, 732–746, 1989.
Geissler, P., and B. Jahne, Laboratory and inshore measurements of bubble size distributions, in *Natural Physical Processes Associated With Sea Surface Sound*, edited by T. G. Leighton, pp. 147–154, CBC Print and Media Resour., Fordingbridge, Hampshire, U.K., 1997.
Gordon, H. R., and A. Morel, *Remote Assessment of Ocean Color for Interpretation of Satellite Visible Imagery-A Review, Lecture Notes on Coastal and Estuarine Studies*, 114 pp., Springer-Verlag, New York, 1983.
Farmer, D. M., and S. Vagle, Bubble measurements using a resonator system, in *Natural Physical Processes Associated With Sea Surface Sound*, edited by T. G. Leighton, pp. 155–162, Univ. of Southampton, Southampton, U.K., 1997.
Farmer, D. M., S. Vagle, A. D. Booth, A free-flooding acoustical resonator for measurement of bubble size distributions, *J. Atmos. Oceanic Tech.*, *15*(5), 1132–1146, 1998.
Lamarre, E., and W. K. Melville, Instrumentation for the measurement of void-fraction in breaking waves–Laboratory and field results, *IEEE J. Ocean Eng.*, *17*, 204–215, 1992.
Loisel, H., and A. Morel, Light scattering and chlorphyll concentration in case 1 waters: A reexamination. *Limnol. Oceanogr.*, *43*(5), 847–858, 1998.
Medwin, H., In situ acoustic measurements of bubble populations in coastal waters, *J. Geophys. Res.*, *75*, 599–611, 1970.
Medwin, H., In situ acoustic measurements of microbubbles at sea, *J. Geophys. Res.*, *82*, 971–976, 1977.
Medwin, H., and N. D. Breitz, Ambient and transient bubble spectral densities in quiescent seas and under spilling breakiers, *J. Acoust. Soc. Am.*, *88*, 408–412, 1989.
Medwin, H., and A. C. Daniel, Acoustical measurements of bubble production by spilling breakers, *J. Acoust. Soc. Am.*, *88*, 812–840, 1990.
Medwin, H., J. Fitzgerald, and G. Rautman, Acoustic miniprobing for ocean microstructure and bubbles, *J. Geophys. Res.*, *80*, 405–413, 1975.
Melville, W. K., The role of surface-wave breaking in air-sea interaction, *Annu. Rev. Fluid. Mech.*, *28*, 279–321, 1996.
Melville, W. K., E. Terrill, and F. Veron, Bubbles and turbulence under breaking waves, in *Natural Physical Processes Associated With Sea Surface Sound*, edited by T. G. Leighton, pp. 135–145, Univ. of Southampton, Southampton, U.K., 1997.
Mobley, C. D., *Light and Water: Radiative Transfer in Natural Waters*, Academic, San Diego, Calif., 1994.

Morel, A., In-water and remote measurements of ocean color, *Boundary Layer Meteorol.*, *18*, 177–201, 1980.

Morel, A., and L. Prieur, Analysis of variations in ocean color, *Limnol. Oceanogr.*, *22*, 709–722, 1977.

O'Hern, T. J., L. D'Agostino, and A. J. Acosta, Comparison of holographic and coulter counter measurements of cavitation nuclei in the ocean, *ASME J. Fluid Eng.*, *110*, 200–207, 1988.

Smith, R. C., and K. S. Baker, Optical properties of the clearest natural waters (200–800 nm), *Appl. Opt.*, *31*, 177–184, 1981.

Stramski, D., Gas microbubbles: An assessment of their significance to light scattering in quiescent seas, *Proc. SPIE Ocean Opt.*, *XII*, *2258*, 704–710, 1994.

Terrill, E. J., Acoustic Measurements of Air Entrainment by Breaking Waves, Ph.D. thesis, 244 pp., Scripps Inst. of Oceanogr., Univ. of Calif., San Diego, La Jolla, 1998.

Terrill, E. J., and W. K. Melville, Sound-speed measurements in the surface wave layer, *J. Acoust. Soc. Am.*, *102*, 2607–2625, 1997.

Terrill, E. J., and W. K. Melville, A broadband acoustic technique for measuring bubble size distributions: Laboratory and shallow water measurements, *J. Atmos. Oceanic Tech.*, *17*, 220–239, 2000.

Terrill, E. J., W. K. Melville, and D. Stramski, Bubble entrainment by breaking waves and their effects on the inherent optical properties of the upper ocean, *Proc. Ocean Opt. OOXIV*, 11 pp., Nov. 1998.

Wildt, R. (Ed.), Physics of sound in the sea, in *Acoustic Theory of Bubbles*, *Summary Tech. Rep. 6*, vol. 8, Natl. Def. Res. Comm., Dep. of Def., Washington, D. C., 1946.

Zhang, X., M. Lewis, and B. Johnson, Influence of bubbles on scattering of light in the ocean, *Appl. Opt.*, *37*, 6525–6536, 1998.

W. K. Melville, E. J. Terrill, and D. Stramski, Scripps Institution of Oceanography, University of California, San Diego, La Jolla, CA 92093-0230.

(Received June 14, 2000; revised April 5, 2001;
accepted April 24, 2001.)